1521-0103/375/1/10–20$35.00
THE JOURNAL OF PHARMACOLOGY AND EXPERIMENTAL THERAPEUTICS

https://doi.org/10.1124/jpet.120.265835
J Pharmacol Exp Ther 375:10–20, October 2020

Dextromethorphan and Dextrorphan Influence Insulin Secretion by Interacting with K_{ATP} and L-type Ca^{2+} Channels in Pancreatic β-Cells[S]

Anne Gresch and Martina Düfer

University of Münster, Pharmaceutical and Medicinal Chemistry, Department of Pharmacology, Münster, Germany

Received February 18, 2020; accepted July 8, 2020

ABSTRACT

The NMDA receptor antagonist dextromethorphan (DXM) and its metabolite dextrorphan (DXO) have been recommended for treatment of type 2 diabetes mellitus because of their beneficial effects on insulin secretion. This study investigates how different key points of the stimulus-secretion coupling in mouse islets and β-cells are influenced by DXM or DXO. Both compounds elevated insulin secretion, electrical activity, and $[Ca^{2+}]_c$ in islets at a concentration of 100 μM along with a stimulating glucose concentration. DXO and DXM increased insulin secretion approximately 30-fold at a substimulatory glucose concentration (3 mM). Patch-clamp experiments revealed that 100 μM DXM directly inhibited K_{ATP} channels by about 70%. Of note, DXM decreased the current through L-type Ca^{2+} channels about 25%, leading to a transient reduction in Ca^{2+} action potentials. This interaction might explain why elevating DXM to 500 μM drastically decreased insulin release. DXO inhibited K_{ATP} channels almost equally. In islets of K_{ATP} channel–deficient sulfonylurea receptor 1 knockout mice, the elevating effects of 100 μM DXM on $[Ca^{2+}]_c$ and insulin release were completely lost. By contrast, 100 μM DXO still increased glucose-stimulated insulin release around 60%. In summary, DXM-induced alterations in stimulus-secretion coupling of wild-type islets result from a direct block of K_{ATP} channels and are partly counteracted by inhibition of L-type Ca^{2+} channels. The stimulatory effect of DXO seems to be based on a combined antagonism on K_{ATP} channels and NMDA receptors and already occurs under resting conditions. Consequently, both compounds seem not to be suitable candidates for treatment of type 2 diabetes mellitus.

SIGNIFICANCE STATEMENT

This study shows that the use of dextromethorphan as an antidiabetic drug can cause unpredictable alterations in insulin secretion by direct interaction with K_{ATP} and L-type Ca^{2+} channels besides its actual target, the NMDA receptor.

Introduction

Dextromethorphan (DXM) is known as a nonopioid over-the-counter cough suppressant. Currently, there are many clinical studies investigating the therapeutic potential of DXM mainly for treatment of diseases related to the central nervous system. Suggested indications are depression, traumatic brain injury, stroke, seizure, pain, methotrexate neurotoxicity, Parkinson disease, and autism (Nguyen et al., 2016). In 2010, the Food and Drug Administration approved the use of DXM in combination with quinidine for patients suffering from pseudobulbar affect. Apart from its neuroprotective properties, DXM has been suggested for treatment of type 2 diabetes mellitus (Marquard et al., 2015, 2016). These versatile effects are based on the antagonism of DXM at the NMDA receptor (NMDAR). The NMDAR is a voltage- and ligand-gated ion channel that opens selectively for cations (especially Na^+, K^+, and Ca^{2+}) upon activation. The heterotetrameric channel is activated by concurrent depolarization to release the Mg^{2+} block out of the pore and by simultaneous binding of its ligand and a coactivator (e.g., glycine) (Vyklicky et al., 2014; Zhu et al., 2016). In the 90s, it became evident that NMDARs exist in insulin-secreting β-cells and take part in the regulation of glucose-induced insulin secretion (Gonoi et al., 1994; Inagaki et al., 1995; Molnar et al., 1995). There are controversial results about the function of NMDARs. Inhibition of the NMDAR either results in increased insulin secretion (Marquard et al., 2015), in no alteration of insulin secretion (Bertrand et al., 1992; Chan et al., 1997; Patterson et al., 2016; Imai et al., 2018; Suwandhi et al., 2018), or in reduced insulin secretion (Patterson et al., 2016). The exact molecular mechanism is not clear yet, but it was demonstrated that NMDAR activity contributes to the trafficking of K_{ATP} channels to the plasma membrane in INS-832/13 cells (Wu et al., 2017). It is conceivable that, as in subthalamic neurons, Ca^{2+} influx through NMDA-gated channels activates K_{ATP} currents through a nitric oxide/cGMP-dependent pathway (Shen and Johnson, 2010). Hence, NMDAR

This work was supported by the Deutsche Forschungsgemeinschaft (Research Training Group GRK 2515, Chemical Biology of Ion Channels).
The authors declare no conflict of interests.
https://doi.org/10.1124/jpet.120.265835.
[S] This article has supplemental material available at jpet.aspetjournals.org.

ABBREVIATIONS: a.u., arbitrary fluorescence unit; Ca_v channel, voltage-regulated Ca^{2+} channel; DXM, dextromethorphan; DXO, dextrorphan; FOPP, fraction of plateau phase; K_{ATP} channel, ATP-dependent K^+ channel; K_{Ca} channel, Ca^{2+}-regulated K^+ channel; Kir6.2, inwardly-rectifying K^+ channel subunit 6.2; K_v channel, voltage-dependent K^+ channel; MEA, microelectrode array; NMDA, *N*-methyl-D-aspartate; NMDAR, NMDA receptor; SUR1-KO, sulfonylurea receptor 1 knockout; V_m, membrane potential.

activation seems to act as a negative-feedback regulator for glucose-induced insulin secretion by promoting K^+ outward currents, which initiate repolarization of the membrane potential. Marquard et al. recommended DXM, or rather its active metabolite dextrorphan (DXO), for treatment of type 2 diabetes mellitus because of its beneficial effects on insulin secretion (Marquard et al., 2015, 2016). Direct effects on important steps of the stimulus-secretion coupling were accomplished with MK-801 (also known as dizocilpine), another noncompetitive NMDAR antagonist. MK-801 changed the pattern of glucose-induced Ca^{2+} oscillations in mouse islets, increased the plateau fraction of Ca^{2+} oscillations, and prolonged the characteristic bursts of electrical activity in glucose-stimulated β-cells (Marquard et al., 2015). However, there is evidence that MK-801 not only blocks NMDAR but also interacts with voltage-dependent K^+ channels (K_v channels). A direct inhibition of K_v channels was shown in dissociated sympathetic neurons and mesenteric arterial smooth muscle cells of rats (Wooltorton and Mathie, 1995; Kim et al., 2015). Several K_v channel subunits that exist in vascular smooth muscle cells are expressed in insulin-secreting cells (MacDonald and Wheeler, 2003). As repolarization of β-cell action potentials is mediated by activation of K_v channels (MacDonald and Wheeler, 2003), the abovementioned effects of MK-801 on Ca^{2+} oscillations might not only be based on interaction with the NMDAR. The aim of this work was to elucidate whether DXM and DXO, respectively, influence insulin secretion by affecting plasma membrane potential and cytosolic Ca^{2+} similar to MK-801. To further investigate whether the observed drug effects are attributable to inhibition of NMDAR and concomitant elimination of its negative feedback on the stimulus-secretion cascade or involve other mechanisms, it was tested whether the two compounds directly interact with K_{ATP} and/or L-type Ca^{2+} channels of primary mouse β-cells.

Methods

Cell and Islet Preparation. Experiments were performed with islets of Langerhans from adult male and female C57BL/6N mice (Charles River, Sulzfeld, Germany). The principles of laboratory animal care were followed according to German laws (Az. 53.5.32.7.1/MS-12668, health and veterinary office Münster, Germany). Breeding pairs of sulfonylurea receptor 1 knockout (SUR1-KO) mice (on a C57BL/6 background) as well as SUR1-KO islets for some initial experiments were kindly provided by Prof. Dr. Gisela Drews (Institute of Pharmacy, Department of Pharmacology and Clinical Pharmacy, University of Tübingen, Germany). Mice were euthanized using CO_2, and pancreatic islets of both genotypes were isolated similarly by collagenase digestion. Murine islets were dispersed to single cells by trypsin-EDTA treatment (0.25%, 2 minutes). Islets or cells were cultured in RPMI 1640 medium (11.1 mM glucose) supplemented with 10% fetal calf serum, 100 U/ml penicillin, and 100 μg/ml streptomycin at 37°C in a 5% CO_2, humidified atmosphere.

Solutions and Chemicals. Electrophysiological measurements and recordings of $[Ca^{2+}]_c$ were performed with a bath solution of (in millimolars) 140 NaCl, 5 KCl, 1.2 $MgCl_2$, 2.5 $CaCl_2$, 10 HEPES, and glucose as indicated (pH 7.4, adjusted with NaOH). For determination of Ca^{2+} currents, the bath solution contained (in millimolars) 115 NaCl, 1.2 $MgCl_2$, 10 $CaCl_2$, 20 tetraethylammonium chloride, 10 HEPES, 15 glucose, and 0.1 tolbutamide (pH 7.4, adjusted with NaOH). Pipette solution for recording of plasma membrane potential (V_m) consisted of (in millimolars) 10 KCl, 10 NaCl, 70 K_2SO_4, 4 $MgCl_2$, 2 $CaCl_2$, 10 EGTA, 5 HEPES, and 0.27 amphotericin B (pH 7.15, adjusted with KOH). For Ca^{2+} currents, the pipette solution was composed of (in millimolars) 50 CsCl, 70 *N*-methyl-D-glucamine, 58 HCl, 4 $MgCl_2$, 2 $CaCl_2$, 10 EGTA, 3 Na_2ATP, and 10 HEPES (pH 7.15, adjusted with CsOH). To determine K_{ATP} currents, pipette solution was composed of (in millimolars) 130 KCl, 4 $MgCl_2$, 2 $CaCl_2$, 10 EGTA, 0.65 Na_2ATP, and 20 HEPES (pH 7.15, adjusted with KOH). Krebs-Ringer-HEPES solution (KRH) for insulin secretion was composed of (in millimolars) 122 NaCl, 4.7 KCl, 1.1 $MgCl_2$, 2.5 $CaCl_2$, 10 HEPES, glucose as indicated, and 0.5% bovine serum albumin (pH 7.4, adjusted with NaOH).

Dextromethorphan hydrobromide was obtained from Alfa Aesar (Thermo Fisher, Karlsruhe, Germany); memantine hydrochloride from Fisher Scientific GmbH (Schwerte, Germany); Collagenase P from Roche Diagnostics (Mannheim, Germany); Corning Matrigel basement membrane preparation from VWR (Darmstadt, Germany); and RPMI 1640, fetal calf serum, and penicillin/streptomycin from Life Technologies (Darmstadt, Germany). Fura-2 acetoxymethylester and rat insulin were ordered from Biotrend (Köln, Germany). Dextrorphan tartrate and all other chemicals were from Sigma-Aldrich (Taufkirchen, Germany) or Diagonal (Münster, Germany).

Insulin Secretion. After preparation, islets were kept overnight in RPMI medium. The next day, medium was removed, and islets were incubated in KRH with 5.6 mM glucose for 1 hour and thereafter in KRH buffer with 3 mM glucose for 0.5 hours. In the case of preincubation, the compounds were already added to the KRH buffer containing 5.6 and 3 mM glucose. For determination of insulin secretion, batches of five islets were incubated at 37°C for 60 minutes with the indicated substances and glucose concentrations. Each condition was prepared in triplicate. For analysis of the kinetics of insulin release, bath chambers were equipped with 50 islets and perfused with KRH at the indicated conditions at a rate of 0.7 ml/min at 37°C. Eluate samples were taken every 2 minutes. Insulin concentration was quantified by a radioimmunoassay using rat insulin as standard. In perfusion experiments, the substimulatory phase was evaluated by determining the area under the curve of a 15-minute time interval. For analysis of glucose-stimulated secretion, the area under the curve was calculated starting from the first rise in insulin release after changing the glucose concentration to 15 mM until the end of the experiment (approximately 50 minutes).

Measurement of $[Ca^{2+}]_c$. For determination of $[Ca^{2+}]_c$, islets were cultured for 1 to 2 days on glass coverslips coated with poly-L-lysine. Islets were loaded with fura-2 acetoxymethylester (5 μM, 37°C, 30 minutes) and thereafter perfused with bath solution plus indicated test substances. Fluorescence was excited at 340 and 380 nm, and emission was measured by a digital camera (filter 515 nm). Alterations in mean $[Ca^{2+}]_c$ were evaluated by calculating the average of the mean Ca^{2+} concentration in bath solution with 3 or 8 mM glucose for 15 minutes (1-hour preincubation experiments), for the last 5 minutes with the respective test compounds (acute application), or for the last 2 minutes in the presence of 0.5 mM glucose. The effect of DXM on the interburst duration was calculated by averaging the two preceding interburst intervals under control conditions in comparison with the period in which $[Ca^{2+}]_c$ remained at the basal niveau after addition of DXM. To confirm that the islets were metabolically intact, bath solution with 0.5 or 8 mM glucose was applied at the end of each experiment. Pancreatic β-cells exhibit characteristic glucose-evoked oscillations, which disappear in the presence of a low glucose concentration (Grapengiesser et al., 1988).

Electrophysiology. Patch-clamp experiments were performed with single islet cells. Pipettes were pulled from borosilicate glass capillaries (resistance of 3–5 MΩ). An EPC-10 patch-clamp amplifier (software "Patchmaster" and "Fitmaster"; HEKA, Germany) was used for data acquisition and analysis. V_m was measured in the current-clamp mode. V_m was evaluated by determination of the plateau potential (from which action potentials start) for a period of 1 minute before changing bath solution. The frequency of action potentials was evaluated during a 4- to 5-minute interval. K_{ATP} current was recorded by application of 300-millisecond pulses to −80 and −60 mV, respectively, starting from a holding potential of −70 mV every

15 seconds. K_{ATP} current was determined for the voltage step from −70 to −60 mV. Ca^{2+} current was recorded by three repetitive 100-millisecond pulses to 0 mV in 3-second intervals, starting from a holding potential of −70 mV every 30 seconds. The peak Ca^{2+} current was analyzed, and the currents of three succeeding pulses for each measuring point were averaged. For current-clamp experiments, cells were identified as β-cells by glucose-dependent appearance of action potentials (see $[Ca^{2+}]_c$ experiments). In current measurements, we used the cell capacitance as a criterion for β-cell identification (Göpel et al., 1999). The mean cell capacitance of all cells selected for analysis was 8 ± 2 pF.

Electrical activity of whole islets was determined by extracellular membrane potential recordings with microelectrode arrays (MEA2100-system with 60MEA200/30iR-Ti-gr and MC-Rack software; Multi Channel Systems, Reutlingen, Germany). Data were low-pass filtered at 25 Hz and sampled at 1000 Hz. Islets were cultured for 3 to 4 days on MEAs coated with Matrigel. Medium was changed to bath solution with 3 mM glucose at the beginning of each experiment. Thereafter, glucose was elevated to 8 mM, followed by the addition of test compounds as indicated. For analysis, the fraction of plateau phase (FOPP, i.e., time with bursting activity related to the entire time interval) was calculated at the end of each experimental maneuver for a period of 20 minutes. Differences in sample sizes are due to the random number of islets attaching on an electrode of the microelectrode array.

Statistics. Data were collected from islets or islet cells of at least three independent mouse preparations for each series of experiments. Values are given as scatter plots and means ± S.D. Data were normally distributed. Statistical significance was assessed by unpaired Student's *t* test (Fig. 2; Fig. 3D), paired Student's *t* test (Fig. 3F; Fig. 4, B and D; Fig. 5, B and G; Fig. 6C), or ANOVA followed by Student-Newman-Keuls post hoc test for multiple comparisons (Fig. 1; Fig. 3B; Fig. 4C; Fig. 5, D and E; Fig. 6A). The null hypothesis of each series of experiments was that the test compound has no influence on the respective parameter. Values of $P \leq 0.05$ were considered statistically significant.

Results

DXM and DXO Increase Insulin Secretion. The influence of the NMDAR antagonists DXM and its metabolite DXO on insulin secretion was investigated in the presence of different glucose concentrations. Islets incubated with 100 μM DXM for 1 hour secreted significantly more insulin during stimulation with 3, 8, 10, or 15 mM glucose compared with control (Fig. 1A). The same effect was evoked by 100 μM DXO, but to achieve this, the incubation time had to be elevated from 1 to 2.5 hours. Most likely, this is due to the higher hydrophilicity of the demethylated compound (Yu and Haining, 2001). In these experiments, islets were already treated with DXO after changing the culture medium (10 mM glucose) to KRH solution with substimulatory glucose concentrations for 1.5 hours prior to the 1-hour stimulation with glucose (Fig. 1B). Neither DXM nor DXO significantly enhanced glucose-stimulated insulin secretion at a lower concentration of 10 μM (Fig. 1, C and D). Basal insulin release was also unaffected by this concentration [3 mM glucose control: 0.07 ± 0.02 ng insulin/(islet*h), +10 μM DXM: 0.06 ± 0.03 ng insulin/(islet*h), $n = 6$, $P = 0.6$, +10 μM DXO: 0.056 ± 0.006, $n = 6$, $P = 0.1$]. Strikingly, and in contrast to DXO, insulin release was even reduced by around 40% by DXM at a concentration of 500 μM (Fig. 1C). As 100 μM DXO and DXM, respectively, stimulated insulin secretion most efficiently in our experiments, we further evaluated how the kinetics of insulin secretion were affected by this concentration. Glucose induces insulin secretion in a biphasic pattern: an initial peak (first phase), which develops rapidly but lasts only a few minutes, followed by a persistent plateau (second phase). DXO and DXM influenced both phases of glucose-induced insulin release. Similar to the effect in static incubations, both compounds substantially elevated insulin secretion at 3 mM glucose (Fig. 1E).

Influence of NMDAR Antagonists on Membrane Potential Oscillations. NMDARs are ligand- and voltage-gated ion channels, which allow the permeation of Ca^{2+} ions. As changes in membrane potential and subsequent Ca^{2+} influx are the key events for regulation of insulin release, we studied the influence of the NMDAR antagonists on electrical activity. Whole pancreatic islets were cultured for 3 to 4 days on microelectrode arrays to achieve a close contact between islet and electrode. The FOPP, i.e., the period islets display bursts of action potentials, was determined at a glucose concentration of 8 mM, which is close to the threshold concentration for activation of mouse islets. At this glucose concentration, the FOPP varied around 10%–20%, and stimulatory effects were easy to detect. The oscillatory pattern induced by 8 mM glucose was changed to permanent depolarization after application of 100 μM DXM (representative experiment shown in Fig. 2A, lower trace). Corresponding to the results observed for insulin secretion, the low concentration of 10 μM DXM elevated the FOPP significantly less than 100 μM DXM (Fig. 2A, upper trace, Fig. 2B, evaluation of all recordings). Similar results were obtained for DXO (Fig. 2, C and D).

Effects of DXM and DXO on $[Ca^{2+}]_c$ in Islets and Single β-Cells. So far, our data support the hypothesis concluded from the experiments with MK-801 (Marquard et al., 2015) that blocking NMDAR augments the glucose-induced depolarization of β-cells. As this is expected to result in a rise in Ca^{2+} influx, we examined whether changes in electrical activity and glucose-induced insulin secretion are correlated to changes in $[Ca^{2+}]_c$. Treatment of whole islets with DXM (100 μM) abolished the typical oscillatory pattern of $[Ca^{2+}]_c$ in the presence of 8 mM glucose and elevated $[Ca^{2+}]_c$ compared with controls (Fig. 3A lower vs. upper part, evaluation of all experiments: Fig. 3B). In these experiments, DXM was added to the bath solution 1 hour before and during the initial part of the recording. Of note, $[Ca^{2+}]_c$ further increased directly after washout of DXM, and sometimes fast oscillations reoccurred. Furthermore, analysis of basal $[Ca^{2+}]_c$ at the end of each experiment, in which glucose concentration was lowered from 8 to 0.5 mM, revealed that $[Ca^{2+}]_c$ decreased as expected but remained on a higher level in those islets exposed to DXM before compared with controls (Fig. 3B). To test whether DXM elevates $[Ca^{2+}]_c$ at a substimulatory glucose concentration, it was added in the presence of 3 mM glucose for 1 hour. Thereafter, the recording was started, and $[Ca^{2+}]_c$ was monitored for 15 minutes with DXM still present (see Fig. 3C, lower trace). This maneuver was followed by the washout of DXM and finally by switching the glucose concentration from 3 to 8 mM to confirm the metabolic integrity of the islets. Evaluation of these data showed that DXM increased the basal $[Ca^{2+}]_c$ (Fig. 3D). Another series of experiments revealed that basal $[Ca^{2+}]_c$ increased in response to acute treatment with DXM (15 minutes), but the effect was much less pronounced (3 mM glucose: $F_{340/380}$: 0.48 ± 0.10 a.u., +100 μM DXM: 0.50 ± 0.11 a.u., $n = 8$, $P = 0.04$, data not shown).

Next, we investigated the acute influence of DXM on $[Ca^{2+}]_c$ in glucose-stimulated islets. Remarkably, DXM (100 μM,

10 minutes) exerted a dual effect on the Ca^{2+} oscillations triggered by 8 mM glucose. Initially, the time $[Ca^{2+}]_c$ remained at the low "interburst" level was prolonged. This was observed consistently: when DXM was added at the beginning, on top of, or at the end of an oscillation. Thereafter, $[Ca^{2+}]_c$ was raised to a plateau with or without small, superimposed oscillations, whereas regular, large oscillations did not reoccur during the application of DXM (Fig. 3E, upper trace). For analysis of the initial effect of DXM, the interburst interval of the glucose-induced oscillations was calculated and compared with the time $[Ca^{2+}]_c$ dropped to the interburst niveau in response to DXM. This period was considerably elevated (control 1.1 ± 0.5 minute vs. DXM 3.4 ± 0.9 minutes, n = 14, P = 0.000001). Evaluation of the last 5 minutes of drug application showed that, similar to the results obtained with preincubated islets, mean $[Ca^{2+}]_c$ was increased in DXM-treated cells versus control (Fig. 3F, left part).

Analogous experiments were performed with DXO. Acute application of 100 μM DXO to islets stimulated by 8 mM glucose slightly elevated mean $[Ca^{2+}]_c$ (Fig. 3E, lower trace, and Fig. 3F, right part), but the effect was substantially lower compared with DXM (last 5 minutes of application of DXO: 1.1 ± 0.2 a.u., n = 17 vs. DXM 1.3 ± 0.2 a.u., n = 14, P = 0.0003). In contrast to DXM, DXO did not prolong the first interburst phase after drug application.

Opposing Effects of DXM and DXO on Membrane Potential in Single β-Cells. The transient inhibition of Ca^{2+} oscillations in response to acute application of DXM was

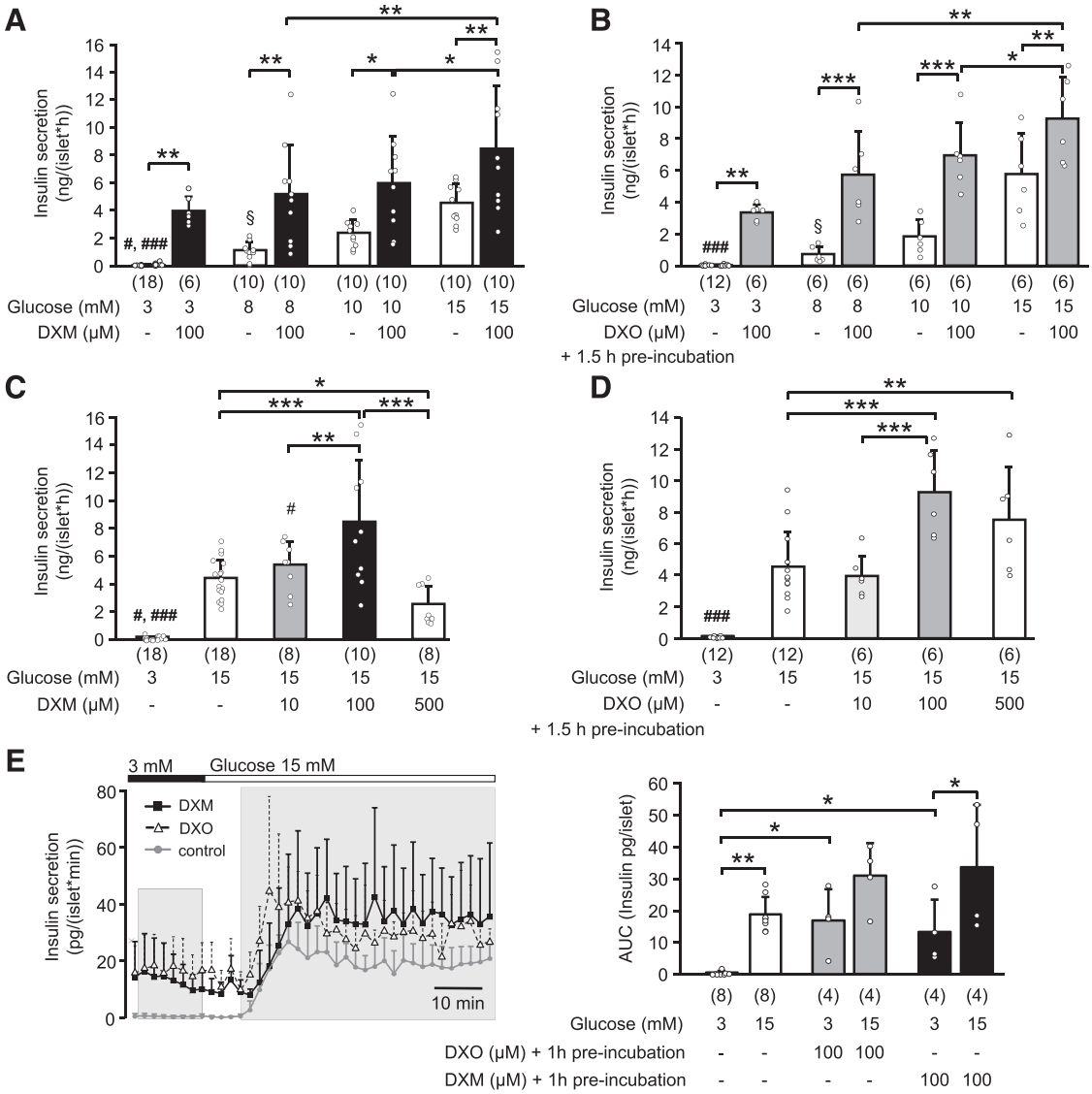

Fig. 1. Effects of DXM and DXO on insulin secretion of mouse islets. (A) Acute treatment (1 hour) with DXM (100 μM) elevates insulin release in the presence of 3, 8, 10, and 15 mM glucose. (B) DXO (100 μM) induces stimulatory effects when exposure time was prolonged to 2.5 hours (1.5 hours preincubation and 1 hour acute application). (C) Insulin secretion (15 mM glucose) is not enhanced by 10 μM DXM but is reduced by 500 μM DXM. (D) Islets stimulated with 15 mM glucose and treated with 10 μM DXO do not show enhanced insulin secretion. (E) DXO and DXM elevate insulin release in the presence of 3 mM glucose and during the first and second phase in response to stimulation with 15 mM glucose (evaluated areas marked in gray). The number of independent islet preparations from different mice is given below each bar. The diagrams in (A–E) summarize the results of all series. Islets were isolated from female/male mice as follows: 10/8 (A), 6/6 (B), 9/9 (C), 5/7 (D), 5/3 (E). $^{*}P \le 0.05$; $^{**}P \le 0.01$; $^{***}P \le 0.001$ as indicated; $^{\#}P \le 0.05$ vs. 10 mM glucose (A) and vs. 500 μM DXM (C); $^{\#\#\#}P \le 0.001$ vs. 15 mM glucose and all conditions with DXM (A and C), DXO (B and D); $^{\S}P \le 0.05$ (A) and $P \le 0.001$ (B) vs. 15 mM glucose. Please note that, for clearness of presentation, only the most relevant significances are included in parts (A, B, and E) of this figure.

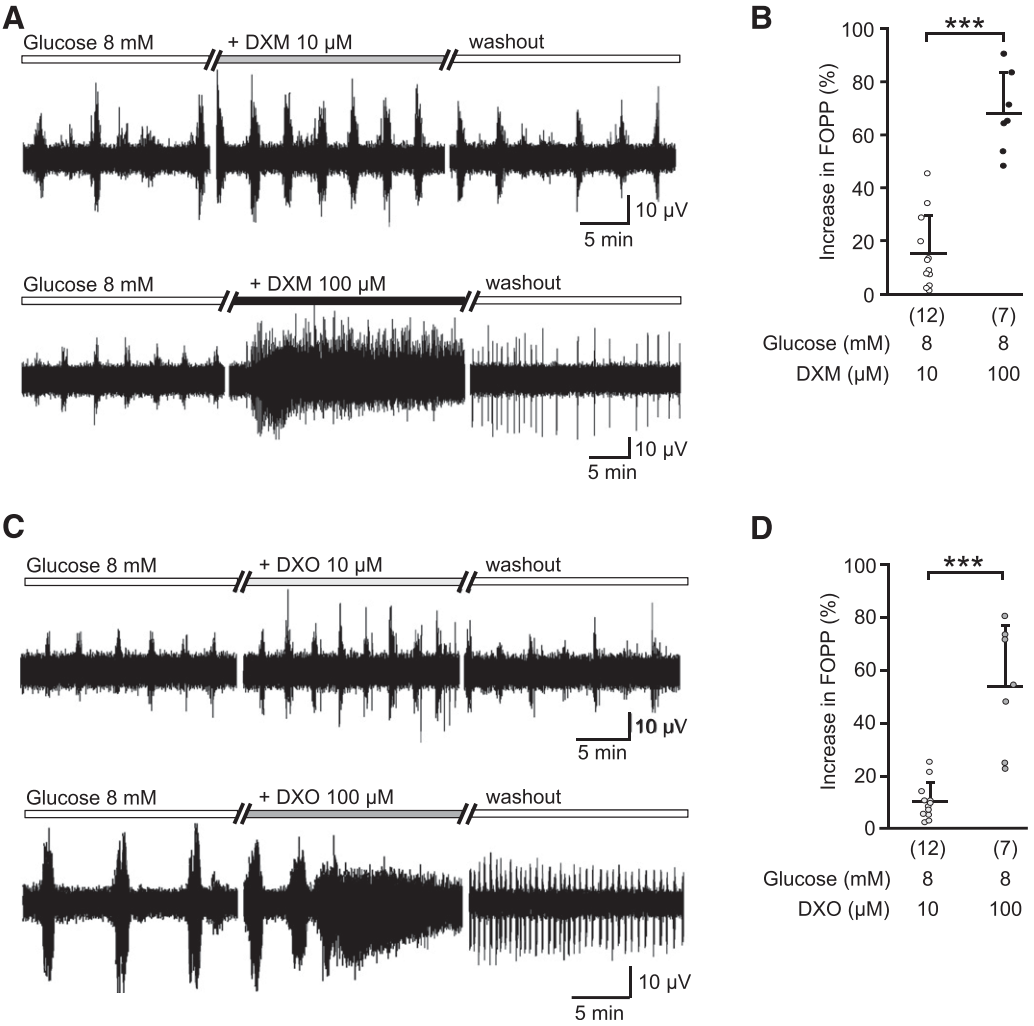

Fig. 2. DXM and DXO increase the electrical activity of whole islets. (A) Representative membrane potential recording of an islet cultured on a microelectrode array. Islets were stimulated with 8 mM glucose and acutely treated with DXM (10 µM upper trace, 100 µM lower trace). (B) Evaluation of all experiments represented in (A). DXM (100 µM) elevates the FOPP considerably more than 10 µM DXM. (C) Same experimental setup as in (A and B) but with DXO instead of DXM. (D) Acute application of DXO (100 µM) elevates the FOPP substantially more than 10 µM DXO. The number in brackets stands for the number of evaluated islets. Islets were isolated from female/male mice as follows: 3/0 (B), 3/0 (D). ***$P \leq 0.001$.

unexpected, as inhibition of NMDAR should dampen the negative feedback of Ca^{2+}-dependent activation of repolarizing currents. Therefore, the influence of DXM on Ca^{2+} action potentials and ion channels was investigated in patch-clamp experiments. In the perforated-patch configuration in which cell metabolism is intact, application of DXM (100 µM) to β-cells stimulated by 8 mM glucose led to an initial reduction in the frequency of action potentials (Fig. 4, A and B). β-Cells were hyperpolarized in one out of six experiments, but overall, V_m was unaffected (control -35 ± 7 mV vs. DXM -31 ± 6 mV, $n = 6$, $P = 0.11$). The inhibiting effect of 100 µM DXM was also present at a glucose concentration of 15 mM. The lower concentration of 10 µM DXM did not affect action potential frequency (Fig. 4C). In agreement with the Ca^{2+} data, there was no negative effect of 100 µM DXO on Ca^{2+} action potentials (Fig. 4D). In summary, these data suggest a direct interaction of DXM with other ion channels apart from NMDAR, e.g., L-type Ca^{2+} channels.

Influence on Ca^{2+} and K_{ATP} Current. To test for direct interactions of the NMDAR antagonists with other ion channels, patch-clamp experiments were performed in the whole-cell configuration, in which cell metabolism is disrupted. The currents were identified as Ca^{2+} currents by application of the L-type Ca^{2+} channel inhibitor nifedipine (10 µM) (Rorsman and Trube, 1986) in each measurement. In agreement with a drop in $[Ca^{2+}]_c$, DXM (100 µM) partially inhibited the Ca^{2+} current (Fig. 5, A and B). Besides a reduction in peak current (Fig. 5B), the decay of the current tended to be faster after application of DXM. This might indicate an influence on channel inactivation (decay time to 63% of the peak current, control: 40 ± 24 milliseconds, $n = 4$, + DXM: 29 ± 13 milliseconds, $n = 5$, $P = 0.39$).

As this result could not explain why the Ca^{2+}-lowering effect was only transient, it was investigated whether DXM also interacts with K_{ATP} channels. It was described that NMDA receptor activity contributes to K_{ATP} channel trafficking and activity, but up to now, there is no information about any direct effects of NMDAR blockers on this ion channel (Shen and Johnson, 2010; Wu et al., 2017). Both compounds, DXM and DXO, inhibited the K_{ATP} current (Fig. 5, C–F). DXM reduced the K_{ATP} current dose-dependently (Fig. 5, C and D). The effect was statistically significant at 50 (control: 20 ± 5 pA/pF vs.

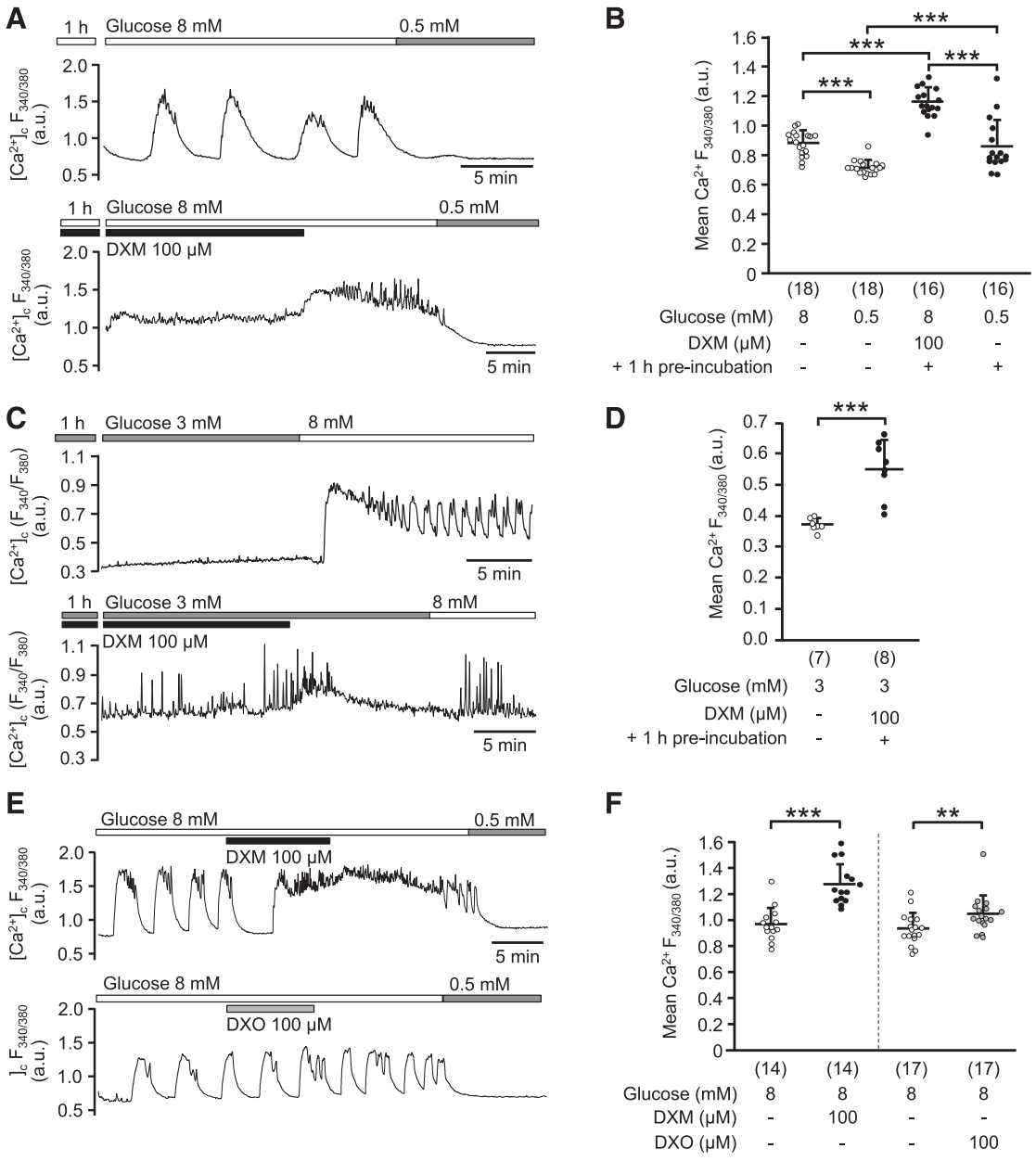

Fig. 3. DXM increases $[Ca^{2+}]_c$ in whole islets. (A) Representative recordings of $[Ca^{2+}]_c$ of an islet stimulated with 8 mM glucose alone (upper trace) or together with 100 µM DXM (lower trace). DXM was present 1 hour before and during the experiment as indicated. (B) Summary of all experiments represented in (A). DXM elevates mean Ca^{2+} at 8 mM glucose in islets after 1 hour of preincubation. Basal Ca^{2+} evaluated at the end of each measurement is also elevated in islets preincubated with 100 µM DXM. (C) DXM elevates mean Ca^{2+} at 3 mM glucose in islets after 1 hour of preincubation. (D) Summary of all experiments presented in (C). (E) Representative recordings of $[Ca^{2+}]_c$ in islets stimulated with 8 mM glucose with acute application of 100 µM DXM (upper trace) or 100 µM DXO (lower trace). Compounds were added 15 minutes after starting the recording. (F) Summary of all experiments represented in (E). Evaluation of the last 5 minutes of treatment with DXM shows a relevant increase of mean $[Ca^{2+}]_c$. Acute application of 100 µM DXO slightly elevates mean $[Ca^{2+}]_c$ of whole islets without an initial drop. The number of evaluated islets (B, D, and F) is given below each data plot. Islets were isolated from female/male mice as follows: 1/2 (B), 1/2 (D), 2/4 (F). $^{**}P \leq 0.01$; $^{***}P \leq 0.001$.

DXM 50 µM: 16 ± 5 pA/pF, $n = 6$, $P = 0.0007$) and 100 µM (control: 24 ± 5 pA/pF vs. DXM 100 µM: 7 ± 4 pA/pF, $n = 5$, $P = 0.001$). After withdrawal of DXM (100 µM), there was a partial recovery in two out of the five experiments, and on average, K_{ATP} current rose to 12 ± 4 pA/pF ($n = 5$, $P = 0.23$ vs. DXM). The inhibitory effect of DXM was not antagonized by 100 µM diazoxide (Fig. 5E) (Dabrowski et al., 2003). DXO (100 µM) also lowered the K_{ATP} current to more than 50% of control (Fig. 5, F and G). This effect was not reversible (8 ± 5 pA/pF, $n = 5$, $P = 0.36$ vs. DXO). Currents were identified as K_{ATP} currents by application of tolbutamide (100 µM) (Trube et al., 1986) in each recording. To elucidate whether direct inhibition of K_{ATP} channels is a side effect shared by other NMDAR blockers, memantine was tested. K_{ATP} current was reduced to approximately 30% by 100 µM of this drug (Supplemental Fig. 1).

Contribution of K_{ATP} Channels to the Rise in Insulin Secretion by DXM and DXO. The data described above show that DXM and DXO directly influence K_{ATP} and Ca^{2+} channels in addition to their well known function as NMDAR

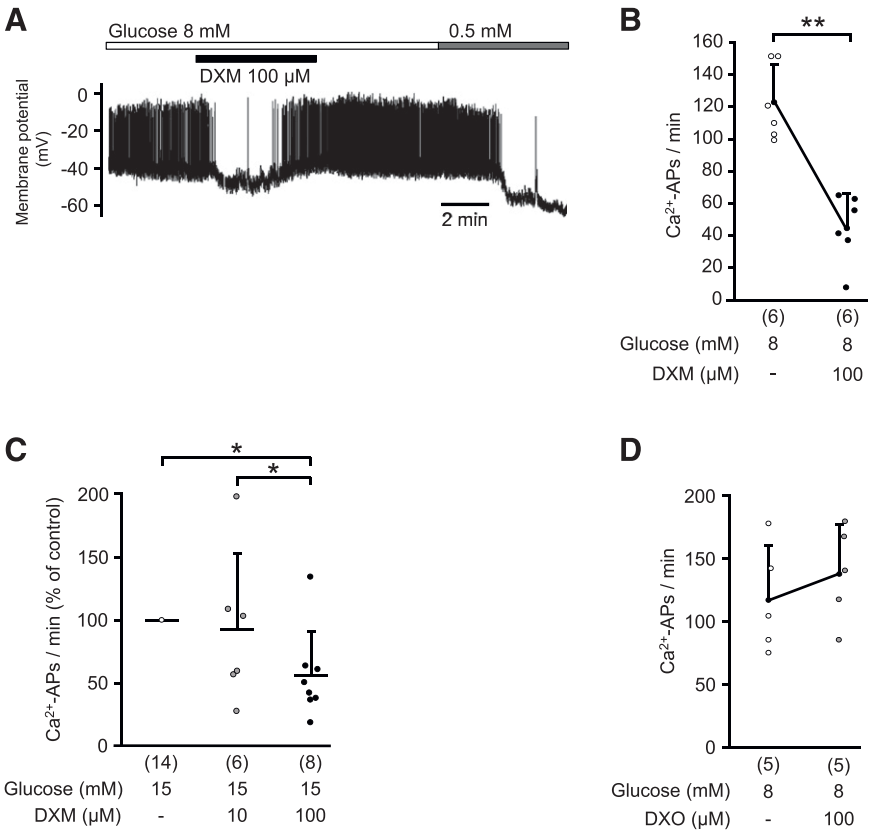

Fig. 4. In contrast to DXO, DXM reduces Ca^{2+} action potentials in glucose-stimulated β-cells. (A) Representative membrane potential recording of a pancreatic β-cell in the perforated-patch configuration. DXM (100 µM) decreases the frequency of action potentials (8 mM glucose). (B) Summary of all experiments represented in (A). (C) Summary of analogous experiments with 15 mM glucose. A lower concentration of DXM (10 µM) does not affect the number of Ca^{2+} action potentials (APs). (D) Similar experiments as in (A) but with DXO. DXO (100 µM) has no effect on Ca^{2+} action potentials. The number in brackets represents the number of experiments with different cells from three mice. Islet cells were isolated from female/male mice as follows: 2/1 (B), 4/3 (C), 2/1 (D). $^*P \leq 0.05$; $^{**}P \leq 0.01$.

antagonists. To investigate the significance of inhibition of K_{ATP} and/or L-type Ca^{2+} channels for modulation of insulin release, we used islets of SUR1-KO mice that do not express functional K_{ATP} channels in their plasma membrane (Seghers et al., 2000). Insulin secretion of SUR1-KO islets stimulated by 15 mM glucose was not elevated by 100 µM DXM (Fig. 6A). $[Ca^{2+}]_c$ measurements with SUR1-KO islets even showed a substantial decrease in mean $[Ca^{2+}]_c$ when DXM was added to the bath solution (Fig. 6B, upper graph, and Fig. 6C, left). This loss of stimulatory effects in SUR1-KO islets demonstrates that inhibition of K_{ATP} channels is the underlying mechanism for the elevation of insulin release by DXM. In comparison, DXO clearly tended to raise insulin secretion in SUR1-KO islets when stimulated with 15 mM glucose (Fig. 6A, grey bar). In addition, determination of the acute effect of DXO on $[Ca^{2+}]_c$ in SUR1-KO islets revealed a slight but statistically significant increase by 100 µM DXO (Fig. 6B, lower graph, and Fig. 6C, right). These data suggest that additional K_{ATP} channel–independent pathways contribute to the insulinotropic effect of DXO.

Discussion

DXM and DXO can increase glucose-induced insulin secretion and were proposed to be potential drugs for treatment of type 2 diabetes mellitus. How NMDAR might modulate β-cell function was investigated with MK-801 (Marquard et al., 2015). Controversial results exist regarding the effect of this compound on insulin release. Although one group (Marquard et al., 2015) detected an elevation of glucose-stimulated insulin secretion, others describe no effect during acute application of MK-801 (Bertrand et al., 1992; Chan et al., 1997; Patterson et al., 2016) or even inhibition after prolonged exposure (Patterson et al., 2016). Consequently, it is difficult to conclude from experiments with MK-801 the mode of action of DXM and DXO. Our results reveal that DXM and its metabolite DXO elevate electrical activity, $[Ca^{2+}]_c$, and insulin secretion. The most efficient concentration in our experiments was 100 µM. This concentration will certainly not be reached in the plasma, but cumulative effects might occur in tissues during long-term use. DXO (10 µM) led to inconclusive results in our study: A rise in secretion was observed in two out of the six mouse preparations, whereas the others showed no or only a negligible response. This result contrasts with Marquard et al. (2015) and cannot be explained by differences in methodology. Of note, Suwandhi et al. (2018) describe a clear stimulatory trend for 10 µM DXO but also no significant effect.

At first glance, our data support the hypothesis that NMDAR antagonists enhance insulin release via the triggering pathway regulated by the plasma membrane potential. Mechanistically, the NMDAR can interact with insulin secretion by several pathways.Wu et al.reported increased trafficking of K_{ATP} and $K_V2.1$ channels to the membrane surface in response to NMDA (Wu et al., 2017). The rise in Ca^{2+} influx via NMDAR could also depolarize mitochondria, thereby increasing the open probability of K_{ATP} channels, as described for Ca^{2+} influx via voltage-regulated Ca^{2+} channels (Ca_v channels) (Drews et al., 2015). Finally, increased local $[Ca^{2+}]_c$ could activate Ca^{2+}-regulated K^+ channels (K_{Ca} channels). Together with the hyperpolarizing current through K_{ATP} channels, opening of K_{Ca} channels is known to initiate the end of each burst phase during the typical oscillations of

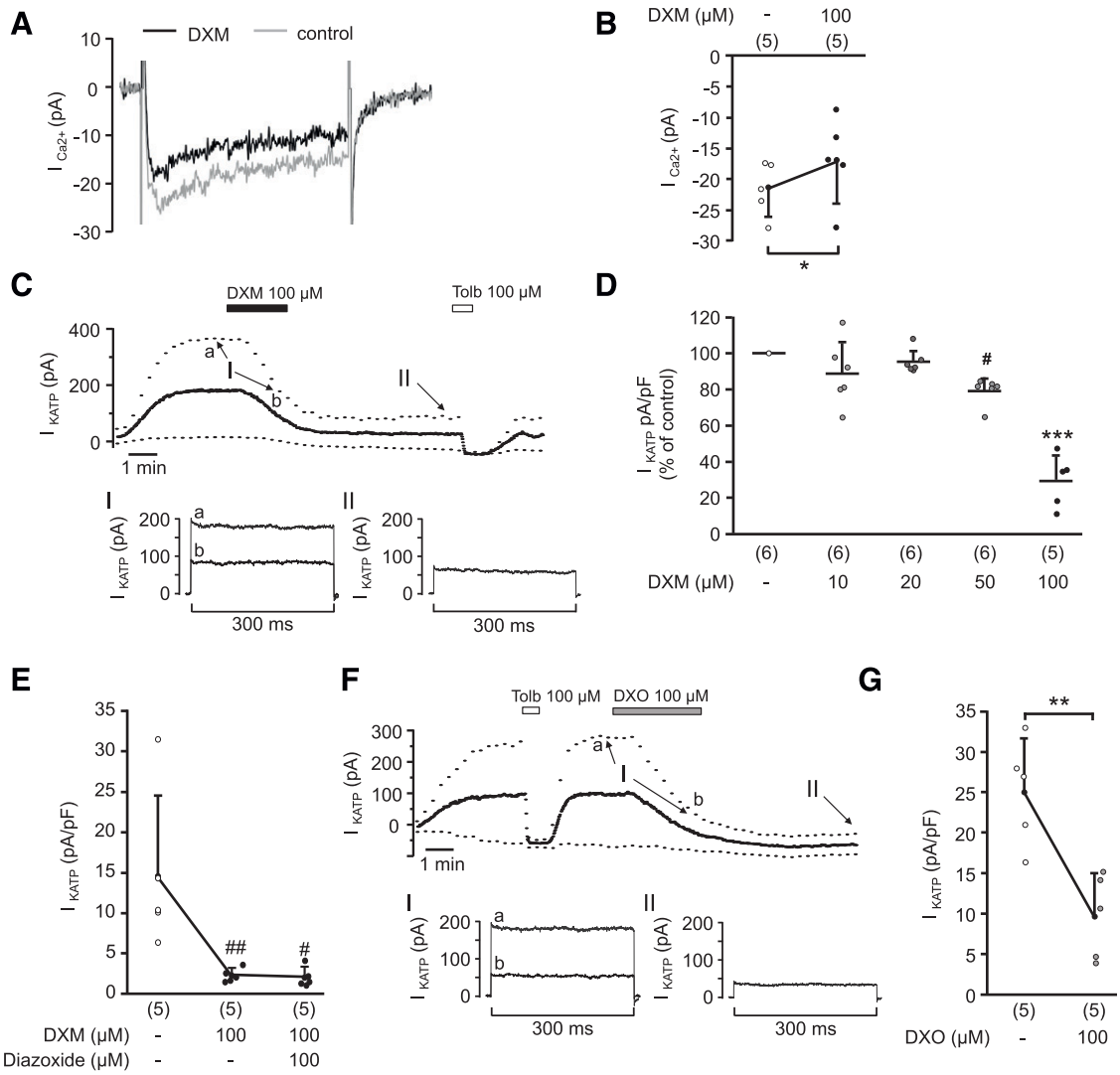

Fig. 5. DXM acutely decreases Ca^{2+} peak currents, and both compounds inhibit K_{ATP} channels of murine β-cells. (A) Representative voltage-clamp recording in the whole-cell configuration shows a decrease of the maximal Ca^{2+} current during administration of DXM (solid, black line) compared with the control condition (solid, gray line). (B) Summary of all experiments represented in (A). DXM (100 μM) reduces the Ca^{2+} current about 25%. (C and F) Representative recordings of K_{ATP} current measured in the whole-cell configuration. Administration of DXM (C) or DXO (F) directly decreases the K_{ATP} current. The current was identified as K_{ATP} current by the specific K_{ATP} channel inhibitor tolbutamide (Tolb; 100 μM). (D) Dose-response curve for the direct effect of DXM (10, 20, 50, and 100 μM) on K_{ATP} current. Statistically significant inhibition occurred with 50 and 100 μM. (E) Lack of antagonism of the DXM-induced inhibition by diazoxide (100 μM). (G) Summary of all experiments with 100 μM DXO. The number in brackets indicates the number of experiments with different cells from three mice. Islet cells were isolated from female/male mice as follows: 4/1 (B), 7/3 (D), 0/3 (E), 3/0 (G). $^{*}P \leq 0.05$; $^{**}P \leq 0.01$; $^{***}P \leq 0.001$ vs. all other conditions, $^{\#}P \leq 0.05$ vs. control and 20 μM DXM, $^{\#\#}P \leq 0.01$ vs. control.

glucose-stimulated pancreatic islets (Düfer et al., 2009; Rorsman and Ashcroft, 2018). Consequently, inhibition of NMDARs should impede repolarization of the β-cell and prolong the burst phases of electrical activity. For MK-801, it was suggested that the stimulatory effect requires K_{ATP} channels (Marquard et al., 2015). To elucidate whether this also applies to DXM and DXO, islets of SUR1-KO mice were used. The two NMDAR antagonists acted differently in K_{ATP} channel–deficient islets. Concomitant with the loss of any positive influence on $[Ca^{2+}]_c$, insulin release was not stimulated by DXM in SUR1-KO islets. By contrast, DXO still elevated $[Ca^{2+}]_c$, although the effect was less pronounced compared with wild-type islets. The effect of DXO on insulin release was more variable in SUR1-KO islets. Stimulation was observed in 7 out of 10 experiments. Statistical significance was reached when tested separately versus control by a Student's *t* test but not in the ANOVA group comparison.

So far, it is obvious that K_{ATP} channels play a central role for the efficacy of DXM and—together with other mechanisms—are involved in the mode of action of DXO. To clarify whether NMDAR is the predominant target for modulation of K_{ATP} channel activity, we investigated the direct influence on other ion channels. Our experiments show for the first time that DXM and DXO both directly inhibit K_{ATP} channels. The effect of DXM was resistant to diazoxide. This differs from the characteristics of established K_{ATP} channel blockers (Rorsman and Trube, 1986) but was reported, e.g., for the experimental compound phentolamine (Plant and Henquin, 1990). As the K_{ATP} channel blockade was very fast and strong, we assume that this direct interaction is much more important for β-cell stimulation than indirect pathways induced by inhibition of NMDAR. Direct inhibition of K^+ currents by DXM was reported for $K_v1.3$ channels (Lee et al., 2011). These channels

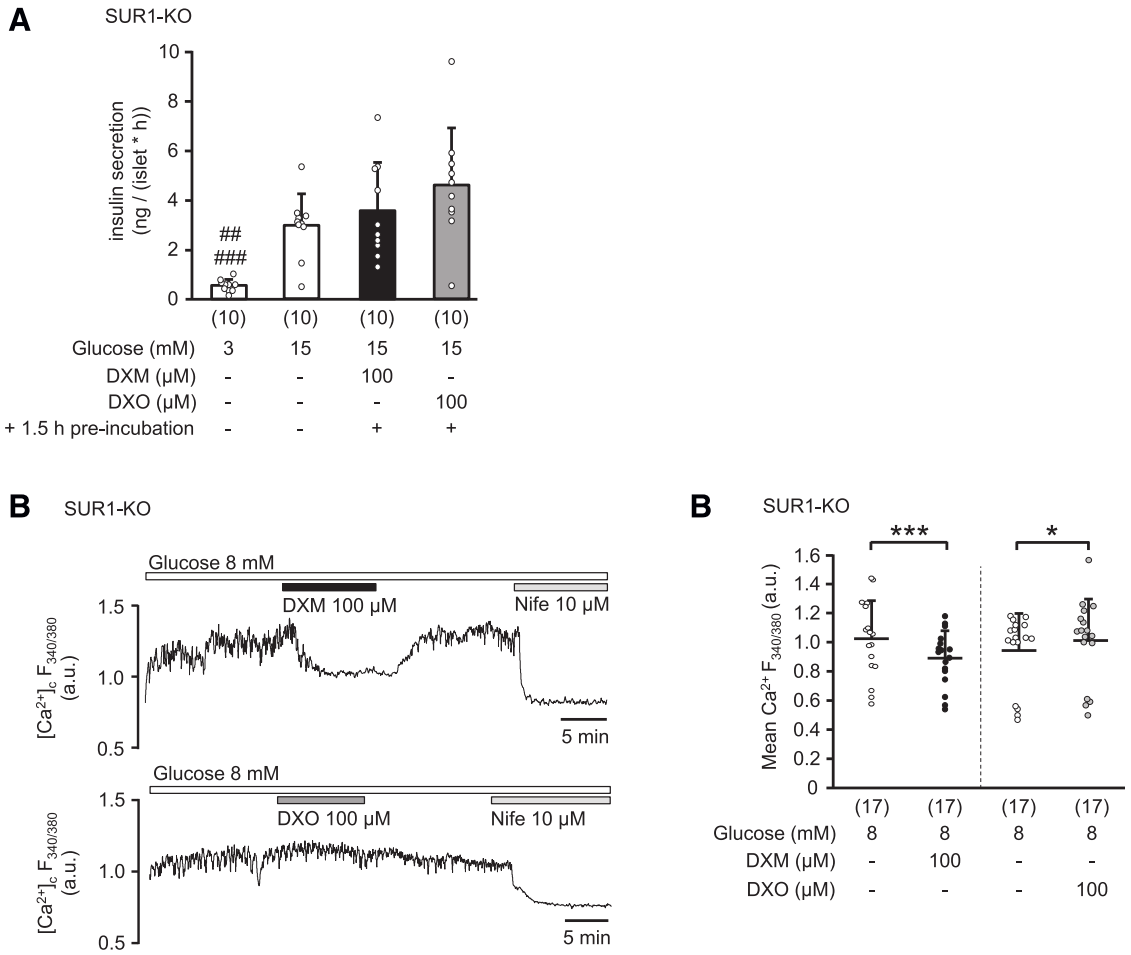

Fig. 6. DXM and DXO affect $[Ca^{2+}]_c$ and insulin release differently in SUR1-KO islets. (A) DXM (100 μM, 1.5 hours of preincubation and 1 hour of acute treatment) does not enhance insulin release (15 mM glucose) of murine SUR1-KO islets, whereas DXO (100 μM, 1.5 hours of preincubation and 1 hour of acute treatment) tends to have an elevating effect. (B) Representative recordings of $[Ca^{2+}]_c$ of SUR1-KO islets stimulated with 8 mM glucose. The upper trace shows a drop in mean Ca^{2+} when DXM is added. By contrast, mean Ca^{2+} slightly rises after addition of DXO (lower trace) Nife: Nifedipine. (C) Summary of all experiments represented in (B). The numbers in brackets indicate independent islet preparations (A) or evaluated islets (C). Islets were isolated from female/male mice as follows: 6/4 (A), 5/2 (C). $^{*}P \leq 0.05$; $^{***}P \leq 0.001$; $^{\#\#}P \leq 0.01$ vs. 15 mM glucose, $^{\#\#\#}P \leq 0.001$ vs. DXO and DXM.

seem to be irrelevant for glucose-stimulated insulin secretion but are associated with regulation of insulin sensitivity (Choi and Hahn, 2010). Taken together, DXM may improve glycemic control by a dual mechanism: an increase in insulin sensitivity and a rise in insulin secretion. In principle, such a combination is not bad, but direct blocking of K_{ATP} channels in β-cells always bears the risk of hypoglycemia. This apprehension is supported by results of Suwandhi et al. (2018), showing a statistically significant membrane depolarization of β-cells with DXO at 2 mM glucose, and by our observation that DXO and DXM extremely elevate insulin release in the presence of 3 mM glucose. DXO stimulates insulin release at this low glucose concentration but is most effective in the presence of 8 and 10 mM glucose. This is in line with a compound inhibiting K_{ATP} channels. At 15 mM glucose, when the majority of K_{ATP} channels is already closed, the effect of channel blockers (sulfonylureas or glinides) is less pronounced (Joost and Hasselblatt, 1979; Ikenoue et al., 1997), similar to our results with DXO.

Apart from the problem of nutrient-independent insulin release, limiting the therapeutic potential of DXM and DXO equally, our study revealed a Ca^{2+}-lowering effect of DXM. The drop in $[Ca^{2+}]_c$ was relatively short and transient in wild-type islets but persisted during the whole application period in sulfonylurea receptor 1–deficient islets. As this is compatible with neither direct inhibition of K_{ATP} channels nor interruption of the indirect negative feedback via NMDAR and K_{ATP} or K_{Ca} channels, DXM must address an additional target. Indeed, we could show that DXM reduces the peak current through L-type Ca^{2+} channels. Inhibition of Ca_v channels by DXM (and DXO) was described for neuronal cells (Carpenter et al., 1988; Netzer et al., 1993). Our patch-clamp recordings, in which intracellular Ca^{2+} was clamped to a low level, suggest an accelerated inactivation by this compound, but further studies are necessary to address this point in detail. Affinity assays showed a 10-fold-higher affinity to Ca_v channels for DXM versus DXO. Furthermore, the affinity of DXM to Ca_v channels is 1.7-fold higher than to NMDARs (Jaffe et al., 1989). In agreement with these differences in the inhibitory potencies, DXM lowered the frequency of Ca^{2+} action potentials in patch-clamped β-cells, whereas DXO neither affected action potentials nor reduced $[Ca^{2+}]_c$. In SUR1-KO islets, DXM lowered $[Ca^{2+}]_c$, but the remaining level was still above basal, and glucose-stimulated insulin release was not

negatively affected. Of note, the high concentration of 500 μM DXM dramatically decreased glucose-stimulated insulin release of wild-type islets. This suggests that the inhibitory effect on L-type Ca^{2+} channels outweighs all other signaling pathways that DXM acts on when the drug accumulates in pancreatic tissue or is severely overdosed.

DXM and DXO also differ in their ability to bind to NMDAR: the affinity of DXO to the NMDAR was reported to be 6.5 times higher compared with DXM (Jaffe et al., 1989), and in contrast to DXM, DXO still raised $[Ca^{2+}]_c$ in SUR1-KO islets. This provides evidence for the potential of NMDAR antagonists to improve β-cell function apart from any (direct or indirect) interaction with K_{ATP} channels. Reduced activation of K_{Ca} channels might play an important role in this scenario. NMDA receptors couple to or are part of a Ca^{2+}-mediated feedback loop with K_{Ca} channels in neurons (Isaacson and Murphy, 2001; Ngo-Anh et al., 2005). One candidate might be the SK4 channel (synonymous. $K_{Ca}3.1$ channel), which is known to be part of the slowly rising K^+ currents terminating burst phases in oscillating β-cells. Eliminating this component of the so-called K_{slow} current dampens the negative-feedback mechanisms maintaining oscillations and elevates $[Ca^{2+}]_c$, thereby fostering insulin release (Düfer et al., 2009). Targeting this pathway has the big advantage that it is not operative under basal $[Ca^{2+}]_c$, i.e., without nutrient stimulation. In this context, it is astonishing that blocking NMDAR by MK-801 was completely ineffective in Kir6.2 knockout islets (Marquard et al., 2015). Possibly, loss of K_{ATP} channels affects the alternative pathways recruited to preserve glucose-regulated hormone secretion differently in the two mouse models. This assumption is supported by the observation that insulin release of islets of Kir6.2 knockout mice is less sensitive to glucose (Miki et al., 1998; Marquard et al., 2015) compared with islets of SUR1-KO mice [Fig. 6 and (Haspel et al., 2005)]. Furthermore, it was shown for β-cells of SUR1-KO mice that K_{Ca} channels could be activated by forced Ca^{2+} influx (Haspel et al., 2005), but it is not known whether this also applies to Kir6.2-deficient β-cells.

DXM was already tested in combination with sitagliptin in a small clinical trial. DXM (independent of dose) numerically reduced maximum blood glucose concentration in response to an oral glucose tolerance test (Marquard et al., 2016). Although the effect was not statistically significant, the results may encourage people to use DXM as an oral antidiabetic drug. Strikingly, development of insulin-dependent diabetes mellitus was reported in a pilot study investigating the therapeutic potential of DXM for treatment of children with severe meningitis (Konrad et al., 2000). With respect to the risk of negative side effects, one can argue that DXO, as the main active metabolite, would be the leading compound reaching the endocrine pancreas. However, it is well known that metabolism of DXM is variable and can occur incompletely. As DXM is metabolized to DXO by CYP2D6 (Yu and Haining, 2001), it accumulates in people with CYP2D6 deficiency due to genetic polymorphisms. A study with 12 healthy volunteers revealed that after ingestion of 25 mg of DXM, the plasma samples of three volunteers exclusively contained DXM, and in another three volunteers, low concentrations of unmetabolized DXM could still be detected (Pfaff et al., 1983). These data underline the unpredictability of metabolism-related drug effects in patients with unknown CYP2D6 status or in patients receiving any CYP2D6-inhibiting drugs.

In summary, our data indicate that the NMDAR influences glucose-mediated stimulus-secretion coupling by K_{ATP} channel–dependent and –independent pathways. With respect to DXM and DXO, the stimulatory mode of action is based on direct inhibition of K_{ATP} channels rather than on NMDAR blockade. To investigate the role of NMDAR in β-cell (patho)physiology and to further elucidate the therapeutic potential of NMDAR inhibitors, novel compounds that, e.g., specifically target NMDAR subunits or are unrelated to the morphinan core structure have to be developed.

Acknowledgments

We thank Julia Kaiser and Jelena Sikimic for preparation of SUR1-KO islets and Melanie Arning and Katrin von Schroetter for skillful technical assistance.

Authorship Contributions

Participated in research design: Gresch, Düfer.

Conducted experiments: Gresch.

Performed data analysis: Gresch.

Wrote or contributed to the writing of the manuscript: Gresch, Düfer.

References

Bertrand G, Gross R, Puech R, Loubatières-Mariani MM, and Bockaert J (1992) Evidence for a glutamate receptor of the AMPA subtype which mediates insulin release from rat perfused pancreas. *Br J Pharmacol* **106**:354–359.

Carpenter CL, Marks SS, Watson DL, and Greenberg DA (1988) Dextromethorphan and dextrorphan as calcium channel antagonists. *Brain Res* **439**:372–375.

Chan SLF, Pallett AL, Clews J, Ramsden CA, and Morgan NG (1997) Evidence that the ability of imidazoline compounds to stimulate insulin secretion is not due to interaction with σ receptors. *Eur J Pharmacol* **323**:241–244.

Choi BH and Hahn SJ (2010) Kv1.3: a potential pharmacological target for diabetes. *Acta Pharmacol Sin* **31**:1031–1035.

Dabrowski M, Larsen T, Ashcroft FM, Bondo Hansen J, and Wahl P (2003) Potent and selective activation of the pancreatic beta-cell type K(ATP) channel by two novel diazoxide analogues. *Diabetologia* **46**:1375–1382.

Drews G, Krippeit-Drews P, and Düfer M (2015) Electrophysiology of islet cells, in *Islets of Langerhans*, 2nd ed. (Islam MS 249–303, Springer Netherlands, Dordrecht, the Netherlands.

Düfer M, Gier B, Wolpers D, Krippeit-Drews P, Ruth P, and Drews G (2009) Enhanced glucose tolerance by SK4 channel inhibition in pancreatic β-cells. *Diabetes* **58**:1835–1843.

Gonoi T, Mizuno N, Inagaki N, Kuromi H, Seino Y, Miyazaki J, and Seino S (1994) Functional neuronal ionotropic glutamate receptors are expressed in the non-neuronal cell line MIN6. *J Biol Chem* **269**:16989–16992.

Göpel S, Kanno T, Barg S, Galvanovskis J, and Rorsman P (1999) Voltage-gated and resting membrane currents recorded from B-cells in intact mouse pancreatic islets. *J Physiol* **521**:717–728.

Grapengiesser E, Gylfe E, and Hellman B (1988) Glucose-induced oscillations of cytoplasmic Ca^{2+} in the pancreatic β-cell. *Biochem Biophys Res Commun* **151**: 1299–1304.

Haspel D, Krippeit-Drews P, Aguilar-Bryan L, Bryan J, Drews G, and Düfer M (2005) Crosstalk between membrane potential and cytosolic Ca^{2+} concentration in beta cells from $Sur1^{-/-}$ mice. *Diabetologia* **48**:913–921.

Ikenoue T, Akiyoshi M, Fujitani S, Okazaki K, Kondo N, and Maki T (1997) Hypoglycaemic and insulinotropic effects of a novel oral antidiabetic agent, (-)-N-(trans-4-isopropylcyclohexanecarbonyl)-D-phenylalanine (A-4166). *Br J Pharmacol* **120**: 137–145.

Imai R, Misaka S, Horita S, Yokota S, O'hashi R, Maejima Y, and Shimomura K (2018) Memantine has no effect on K_{ATP} channels in pancreatic β cells. *BMC Res Notes* **11**:614.

Inagaki N, Kuromi H, Gonoi T, Okamoto Y, Ishida H, Seino Y, Kaneko T, Iwanaga T, and Seino S (1995) Expression and role of ionotropic glutamate receptors in pancreatic islet cells. *FASEB J* **9**:686–691.

Isaacson JS and Murphy GJ (2001) Glutamate-mediated extrasynaptic inhibition: direct coupling of NMDA receptors to $Ca^{(2+)}$-activated K^+ channels. *Neuron* **31**: 1027–1034.

Jaffe DB, Marks SS, and Greenberg DA (1989) Antagonist drug selectivity for radioligand binding sites on voltage-gated and *N*-methyl-D-aspartate receptor-gated Ca^{2+} channels. *Neurosci Lett* **105**:227–232.

Joost HG and Hasselblatt A (1979) Insulin release by tolbutamide and glibenclamide. A comparative study on the perfused rat pancreas. *Naunyn Schmiedebergs Arch Pharmacol* **306**:185–188.

Kim JM, Park SW, Lin HY, Shin KC, Sung DJ, Kim JG, Cho H, Kim B, and Bae YM (2015) Blockade of voltage-gated K^+ currents in rat mesenteric arterial smooth muscle cells by MK801. *J Pharmacol Sci* **127**:92–102.

Konrad D, Sobetzko D, Schmitt B, and Schoenle EJ (2000) Insulin-dependent diabetes mellitus induced by the antitussive agent dextromethorphan. *Diabetologia* **43**:261–262.

Lee J-H, Choi S-H, Shin T-J, Lee B-H, Hwang S-H, Kim H-C, and Nah S-Y (2011) Effect of dextromethorphan on human $K_{(v)}1.3$ channel activity: involvement of C-type inactivation. *Eur J Pharmacol* **651**:122–127.
MacDonald PE and Wheeler MB (2003) Voltage-dependent $K^{(+)}$ channels in pancreatic beta cells: role, regulation and potential as therapeutic targets. *Diabetologia* **46**:1046–1062.
Marquard J, Otter S, Welters A, Stirban A, Fischer A, Eglinger J, Herebian D, Kletke O, Klemen MS, Stožer A, et al. (2015) Characterization of pancreatic NMDA receptors as possible drug targets for diabetes treatment. *Nat Med* **21**:363–372.
Marquard J, Stirban A, Schliess F, Sievers F, Welters A, Otter S, Fischer A, Wnendt S, Meissner T, Heise T, et al. (2016) Effects of dextromethorphan as add-on to sitagliptin on blood glucose and serum insulin concentrations in individuals with type 2 diabetes mellitus: a randomized, placebo-controlled, double-blinded, multiple crossover, single-dose clinical trial. *Diabetes Obes Metab* **18**:100–103.
Miki T, Nagashima K, Tashiro F, Kotake K, Yoshitomi H, Tamamoto A, Gonoi T, Iwanaga T, Miyazaki J, and Seino S (1998) Defective insulin secretion and enhanced insulin action in K_{ATP} channel-deficient mice. *Proc Natl Acad Sci USA* **95**: 10402–10406.
Molnár E, Váradi A, McIlhinney RA, and Ashcroft SJ (1995) Identification of functional ionotropic glutamate receptor proteins in pancreatic β-cells and in islets of Langerhans. *FEBS Lett* **371**:253–257.
Netzer R, Pflimlin P, and Trube G (1993) Dextromethorphan blocks N-methyl-D-aspartate-induced currents and voltage-operated inward currents in cultured cortical neurons. *Eur J Pharmacol* **238**:209–216.
Ngo-Anh TJ, Bloodgood BL, Lin M, Sabatini BL, Maylie J, and Adelman JP (2005) SK channels and NMDA receptors form a Ca^{2+}-mediated feedback loop in dendritic spines. *Nat Neurosci* **8**:642–649.
Nguyen L, Thomas KL, Lucke-Wold BP, Cavendish JZ, Crowe MS, and Matsumoto RR (2016) Dextromethorphan: an update on its utility for neurological and neuropsychiatric disorders. *Pharmacol Ther* **159**:1–22.
Patterson S, Irwin N, Guo-Parke H, Moffett RC, Scullion SM, Flatt PR, and McClenaghan NH (2016) Evaluation of the role of N-methyl-D-aspartate (NMDA) receptors in insulin secreting beta-cells. *Eur J Pharmacol* **771**:107–113.
Pfaff G, Briegel P, and Lamprecht I (1983) Inter-individual variation in the metabolism of dextromethorphan. *Int J Pharm* **14**:173–189.
Plant TD and Henquin JC (1990) Phentolamine and yohimbine inhibit ATP-sensitive K^+ channels in mouse pancreatic β-cells. *Br J Pharmacol* **101**:115–120.
Rorsman P and Ashcroft FM (2018) Pancreatic β-cell electrical activity and insulin secretion: of mice and men. *Physiol Rev* **98**:117–214.
Rorsman P and Trube G (1986) Calcium and delayed potassium currents in mouse pancreatic β-cells under voltage-clamp conditions. *J Physiol* **374**:531–550.
Seghers V, Nakazaki M, DeMayo F, Aguilar-Bryan L, and Bryan J (2000) Sur1 knockout mice. A model for K(ATP) channel-independent regulation of insulin secretion. *J Biol Chem* **275**:9270–9277.
Shen K-Z and Johnson SW (2010) Ca^{2+} influx through NMDA-gated channels activates ATP-sensitive K^+ currents through a nitric oxide-cGMP pathway in subthalamic neurons. *J Neurosci* **30**:1882–1893.
Suwandhi L, Hausmann S, Braun A, Gruber T, Heinzmann SS, Gálvez EJC, Buck A, Legutko B, Israel A, Feuchtinger A, et al. (2018) Chronic d-serine supplementation impairs insulin secretion. *Mol Metab* **16**:191–202.
Trube G, Rorsman P, and Ohno-Shosaku T (1986) Opposite effects of tolbutamide and diazoxide on the ATP-dependent K^+ channel in mouse pancreatic β-cells. *Pflugers Arch* **407**:493–499.
Vyklicky V, Korinek M, Smejkalova T, Balik A, Krausova B, Kaniakova M, Lichnerova K, Cerny J, Krusek J, Dittert I, et al. (2014) Structure, function, and pharmacology of NMDA receptor channels. *Physiol Res* **63** (Suppl 1):S191–S203.
Wooltorton JRA and Mathie A (1995) Potent block of potassium currents in rat isolated sympathetic neurones by the uncharged form of amitriptyline and related tricyclic compounds. *Br J Pharmacol* **116**:2191–2200.
Wu Y, Fortin DA, Cochrane VA, Chen P-C, and Shyng S-L (2017) NMDA receptors mediate leptin signaling and regulate potassium channel trafficking in pancreatic β-cells. *J Biol Chem* **292**:15512–15524.
Yu A and Haining RL (2001) Comparative contribution to dextromethorphan metabolism by cytochrome P450 isoforms in vitro: can dextromethorphan be used as a dual probe for both CTP2D6 and CYP3A activities? *Drug Metab Dispos* **29**:1514–1520.
Zhu S, Stein RA, Yoshioka C, Lee C-H, Goehring A, Mchaourab HS, and Gouaux E (2016) Mechanism of NMDA receptor inhibition and activation. *Cell* **165**:704–714.

Address correspondence to: Dr. Martina Düfer, Pharmaceutical and Medicinal Chemistry, Department of Pharmacology, PharmaCampus, Corrensstraße 48, 48149 Münster, Germany. E-mail: martina.duefer@uni-muenster.de

Supplemental Information

Article: Dextromethorphan and dextrorphan influence insulin secretion by interacting with K_{ATP} and L-type Ca^{2+} channels in pancreatic β-cells

Authors: Anne Gresch, Martina Düfer

Journal: The Journal of Pharmacology and Experimental Therapeutics

Supplemental Figure 1

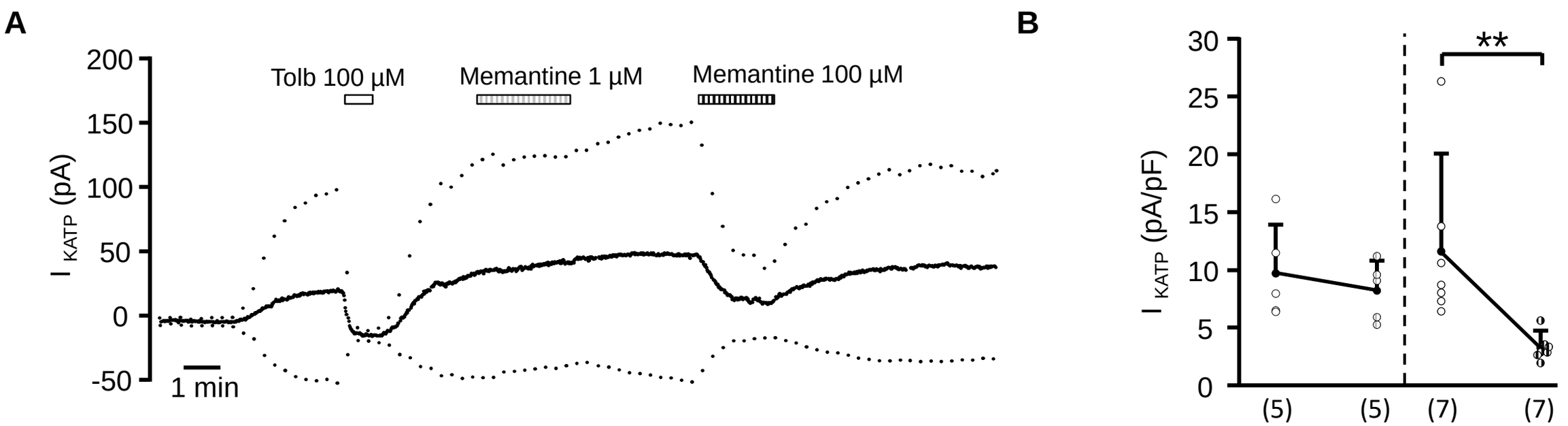

Supplemental Figure 1: Memantine (100 µM) acutely decreases K_{ATP} currents of murine β-cells. A) Representative recording of K_{ATP} current measured in the whole-cell configuration. Administration of 1 µM memantine had no effect while 100 µM decreased the K_{ATP} current. The current was identified as K_{ATP} current by the specific K_{ATP} channel inhibitor tolbutamide (100 µM). B) Summary of all experiments. Different concentrations were not always applied in the same recording. The number in brackets indicates the number of experiments with different cells from 3 mice. Islets were isolated from female/male mice as follows: 2/1 (B). **p≤0.01.